

## Supplementary Materials for

### **Direct visualization of the thermomagnetic behavior of pseudo–single-domain magnetite particles**

Trevor P. Almeida, Adrian R. Muxworthy, András Kovács, Wyn Williams, Paul D. Brown, Rafal E. Dunin-Borkowski

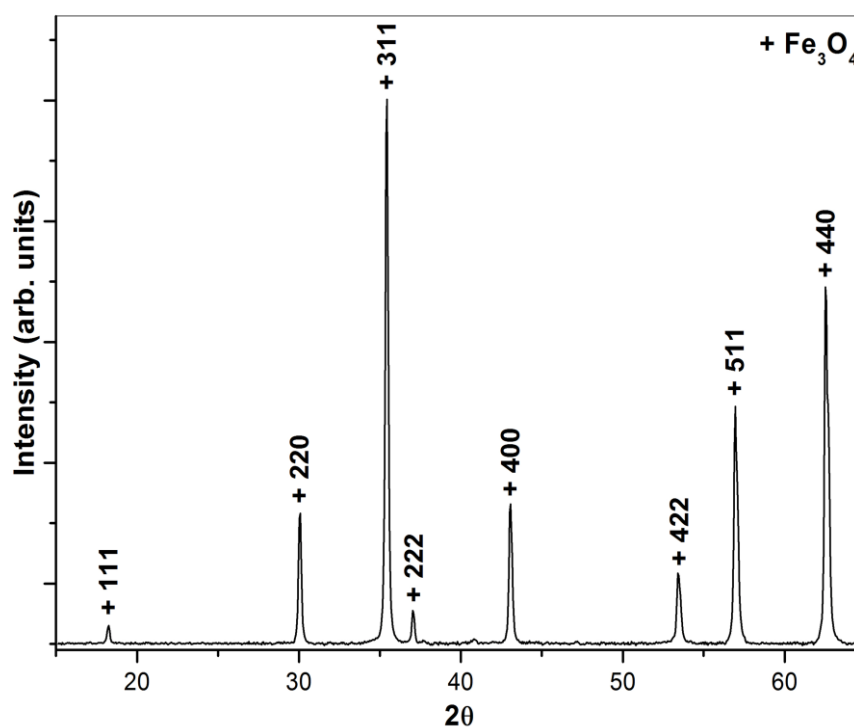
Published 15 April 2016, *Sci. Adv.* **2**, e1501801 (2016)  
DOI: 10.1126/sciadv.1501801

#### **This PDF file includes:**

- X-ray diffractometry
- In situ heating within the TEM
- Off-axis electron holography
- fig. S1. X-ray diffraction pattern of the Fe<sub>3</sub>O<sub>4</sub> powder.
- fig. S2. Images of DENSolutions Wildfire in situ heating holder and EMheaterchips.
- fig. S3. Schematic diagram of the setup for off-axis electron holography.
- fig. S4. Magnetic induction maps of sample G1 at intermediate stages of heating and cooling.
- fig. S5. Magnetic induction maps and proposed 3D forms of vortex states in sample G1.
- fig. S6. Magnetic induction maps of sample G2 at intermediate stages of heating and cooling.
- fig. S7. Magnetic induction maps and proposed 3D forms of vortex states in sample G2.

## X-ray diffractometry

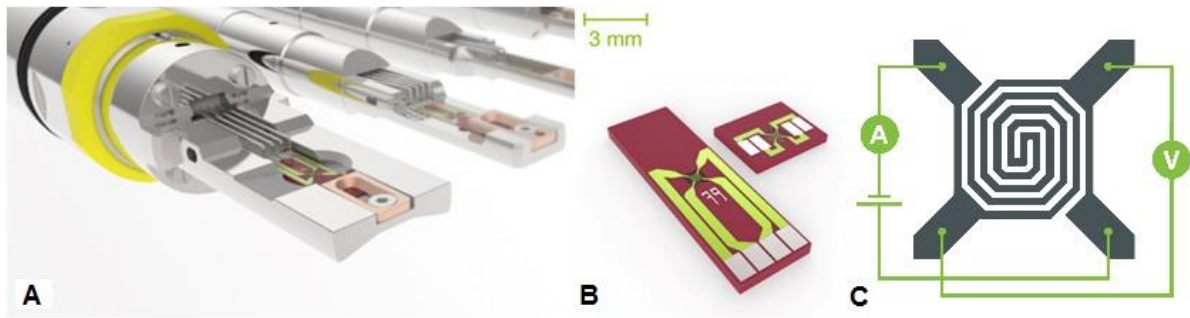
The  $\text{Fe}_3\text{O}_4$  powder was deposited onto a single crystal silicon substrate for crystallographic examination using X-ray diffractometry (PANalytical X'Pert PRO Diffractometer). The XRD pattern of fig. S1 provides information on the crystal structure of the synthesized  $\text{Fe}_3\text{O}_4$  powder. The peaks are in agreement with the presence of  $\text{Fe}_3\text{O}_4$  (Joint Committee on Powder Diffraction standards (JCPDS) reference 75-449).



**fig. S1.** X-ray diffraction pattern of the synthesized powder, confirming the magnetite  $\text{Fe}_3\text{O}_4$  phase (indexed, JCPDS 75-449).

## In situ heating within the TEM

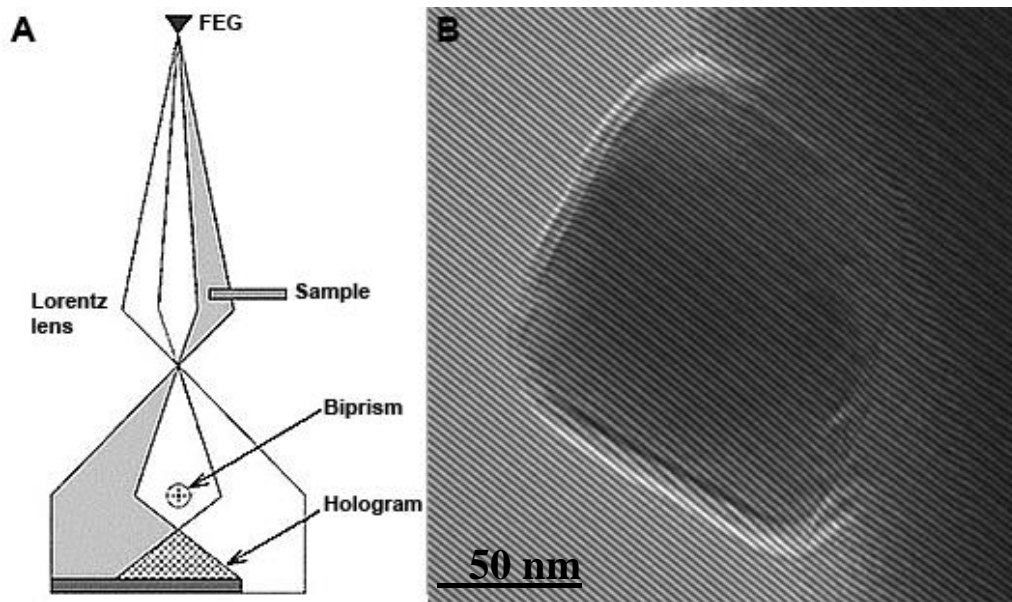
In order to perform in situ heating within the TEM, whilst maintaining stability and minimising thermal drift, a DENSolutions Wildfire in situ heating TEM holder (fig. S2a), which incorporates the EMheaterchip<sup>TM</sup> technology (fig. S2b), was used. The EMheaterchips<sup>TM</sup> are based on Micro-Electro-Mechanical Systems (MEMS) which comprise very small heating elements that provide targeted heating (fig. S2c).



**fig. S2.** Images of DENSsolutions (A) Wildfire in situ heating holder; (B) EMheaterchips™; and (C) MEMS-based heating element.

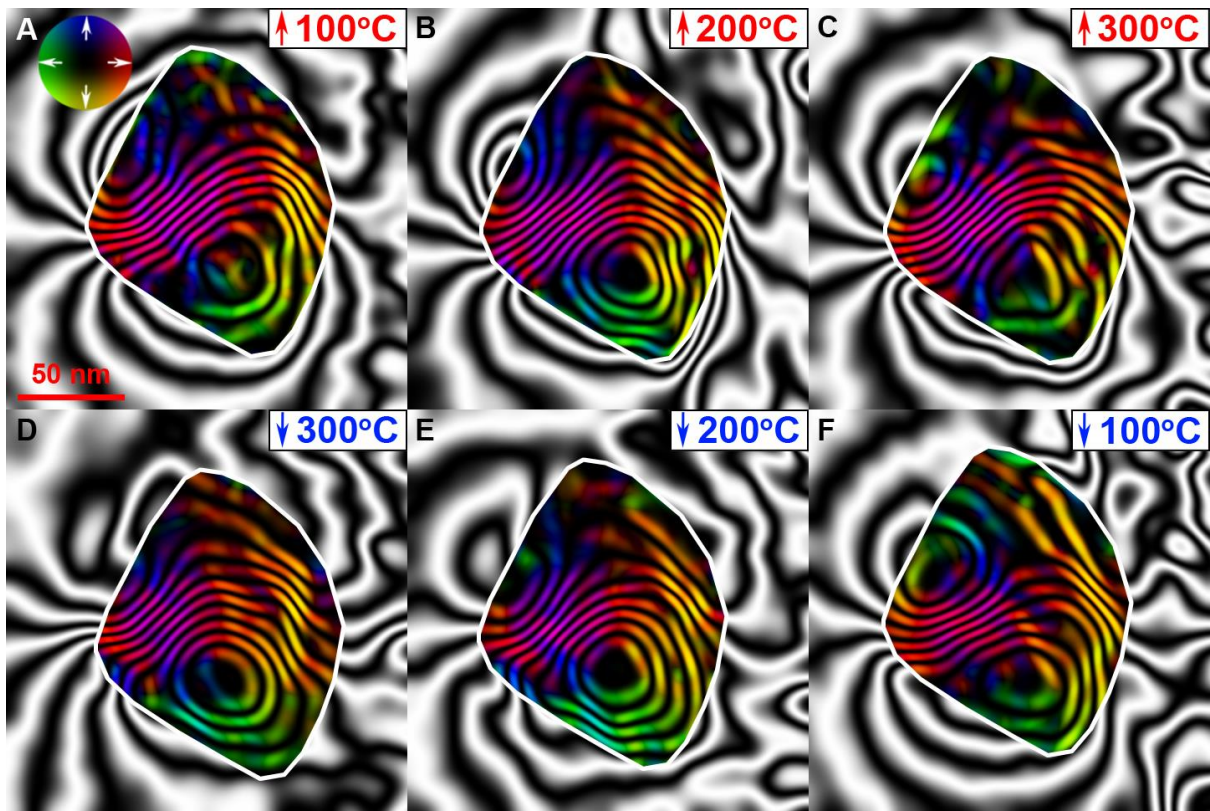
### Off-axis electron holography

Electron holography is a TEM technique that provides direct access to the phase shift of the electron wave that has passed through a thin specimen and allows for imaging of the in-plane magnetic induction. The technique is illustrated schematically in fig. S3A where a biprism (a thin conducting wire) has a positive voltage applied to it in order to overlap a "reference" electron wave (passed through vacuum) with the electron wave that has passed through the specimen (10). The overlap region contains interference fringes and an image of the specimen (fig. S3B), with the fringes possessing information on the phase shift experienced by the electron wave, which is sensitive to both the electrostatic potential and the in-plane component of the magnetic induction in the specimen. In common practice, isolation of the magnetic contribution to the phase shift is achieved through reversal of the direction of magnetization in situ in the TEM, by tilting the sample to equal and opposite high angle tilt angles and turning on the conventional microscope objective lens to apply a strong magnetic field, parallel to the direction of the electron beam. The objective lens is then turned off and the sample tilted back to  $0^\circ$  for hologram acquisition in field-free conditions with the sample at remanence of saturation magnetization.



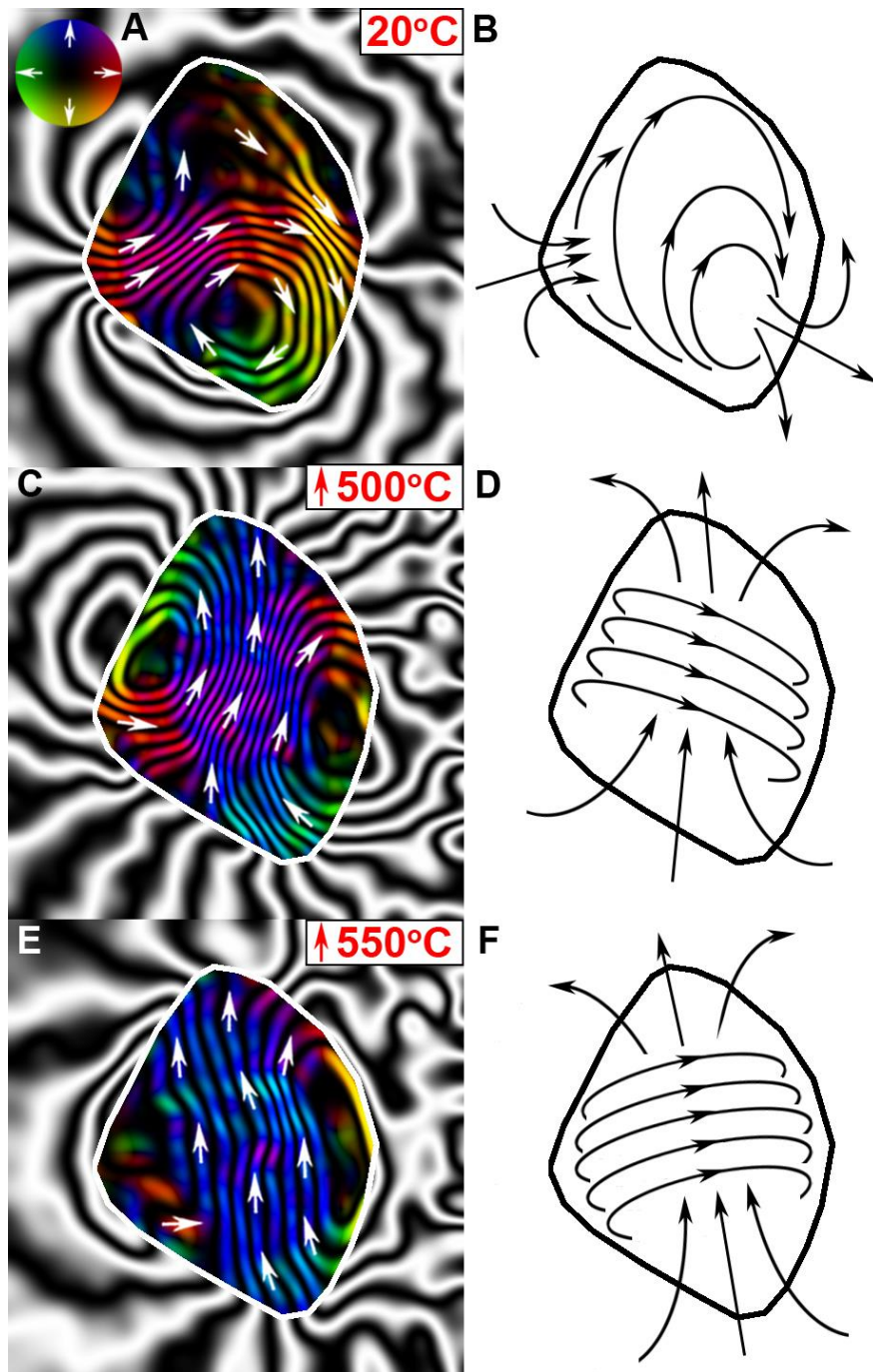
**fig. S3.** (A) Schematic diagram of the setup for off-axis electron holography; and (B) an electron hologram of sample G1, showing well resolved interference fringes from which the phase shift is calculated.

fig. S4 presents the additional temperature interval steps of 100°C, 200°C and 300°C for the thermomagnetic sequence of sample G1 during in situ heating (fig. S4, A-C) and cooling (fig. S4, D-F).



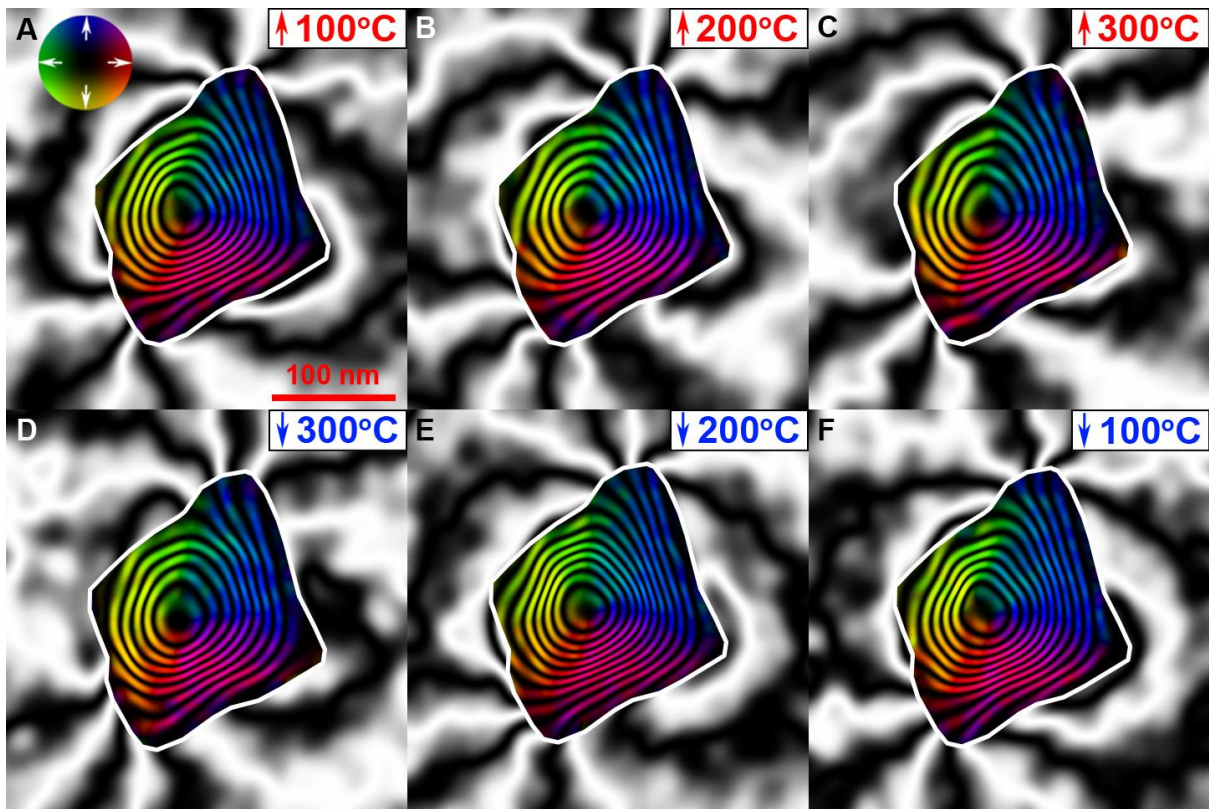
**fig. S4.** (A-F) Magnetic induction maps of sample G1 shown in Fig. 1, reconstructed from holograms taken during in situ heating to (A) 100°C; (B) 200°C; and (C) 300°C; as well as upon cooling from 550°C to (D) 300°C; (E) 200°C; and (F) 100°C. The contour spacing is 0.098 radians for all the magnetic induction maps and the magnetization direction is shown using arrows, as depicted in the colour wheel. The sample was initially magnetically saturated at room temperature.

fig. S5 presents the magnetic induction maps of sample G1 and schematic diagrams of proposed 3D forms of the vortex-like magnetic states that are observed experimentally in projection at 20°C (fig. S5, A&B), 500°C (fig. S5, C&D) and (fig. S5, E&F).



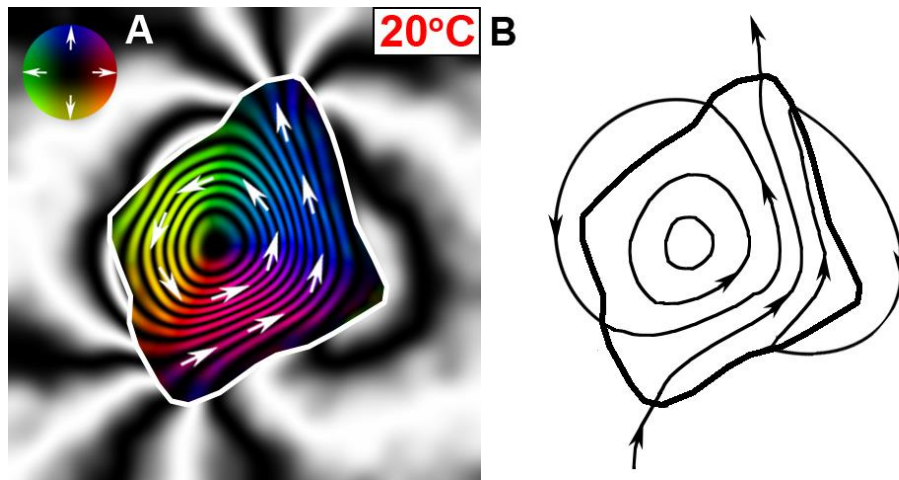
**fig. S5.** (A, C, E) Magnetic induction maps of sample G1 reconstructed from holograms taken at (A) 20°C; and during in situ heating to (C) 500°C; and (E) 550°C. (B, D, F) Schematic representations of the proposed 3D forms of the vortex-like magnetic states observed experimentally in projection at (B) 20°C; (D) 500°C; and (F) 550°C.

fig. S6 presents the additional temperature interval steps of 100°C, 200°C and 300°C for the thermomagnetic sequence of sample G2 during in situ heating (fig. S6, A-C) and cooling (fig. S6, D-F).



**fig. S6.** (A-F) Magnetic induction maps of sample G2 shown in Fig. 2, reconstructed from holograms taken during in situ heating to (A) 100°C; (B) 200°C; and (C) 300°C; as well as upon cooling from 550°C to (F) 300°C; (G) 200°C; and (H) 100°C. The contour spacing is 0.53 radians for all the magnetic induction maps and the magnetization direction is shown using arrows, as depicted in the colour wheel. The sample was initially magnetically saturated at room temperature.

fig. S7 presents the magnetic induction map of sample G2 at 20°C (fig. S7A) and a schematic diagram of the proposed 3D form of the vortex-like magnetic state observed experimentally in projection (fig. S7B).



**fig. S7.** (A) Magnetic induction map of sample G2 reconstructed from holograms taken at 20°C; and (B) schematic representation of the proposed 3D form of the vortex-like magnetic state observed experimentally in projection.